Characterization of Bacterial Cellulose-Chitosan Composite Membrane Grafted With Theophylline-Imprinted Copolymer

Mohd Redza Abd Rahman, Ida Idayu Muhamad, Siti Nur Hidayah Mohamad, and Norhayati Pa'e*

Dept. of Bioprocess Engineering, Faculty of Chemical Engineering, Universiti Teknologi Malaysia Johor Bahru 81310 Johor, Malaysia

Received: 29 January 2013, Accepted: 23 April 2013

SUMMARY

Benzyl diethyldithiocarbamate is immobilized on a composite bacterial cellulose-chitosan membrane via a silane coupler. This treated membrane is grafted with theophylline-imprinted copolymer of methacrylic acid and ethylene glycol dimethacrylate by ultraviolet irradiation. The highest degree of grafting obtained is 0.3334% for r (weight ratio of monomers to bacterial cellulose-chitosan membrane) equal to 3.244 in mmol/ml. The synthesized membrane is prepared by using 0.5% chitosan solution containing 15.0% PEG and evaporating the solution for 2.5 hour after coating at room temperature. The relative flux of 3.69 L/m^2.h at 12.5 bar is obtained. The average pore diameters are 135 Å in dry state and 404 Å in wet state. The chitosan and polyethylene glycol contents have a significant effect on membrane porosity and the flow rate of water through the membrane. The membrane tensile strength is larger than the plain bacterial cellulose support, in both wet and dry states.

KEYWORDS: Bacterial-cellulose chitosan, Membrane, Theophylline, Molecularly imprinted polymers, Grafting

INTRODUCTION

In nature, most biological processes are governed by mechanisms for molecular recognition. These include the immuno response, the ligand-

*Corresponding author: Ida Idayu Muhamad.
Email: idayu@cheme.utm.my

receptor interaction, and enzyme catalysis. They involve such biological hosts as antibodies, enzymes or receptors strongly and specifically binding to a particular molecular structure. To this end, many synthetic low molecular weight organic receptors capable of encapsulating reagents have been designed [1]. The construction of such receptors, however, usually requires complicated multi-step synthesis, which severely limits their large-scale application. Developing other synthetically more accessible receptors is thus highly desirable. Interest in a new class of artificial receptors, molecularly imprinted polymers (MIPs), has increased rapidly in recent years because of their easy preparation, thermal and chemical stability, and highly selective recognition capabilities [2]. MIPs can be synthesized by conventional radical copolymerization of crosslinking monomers and functional monomers which can form reversible complexes with template molecules [3].

Nowadays, the molecular imprinting technique has become a straightforward and versatile method for the generation of molecular imprinting process is its generality, which offers the freedom to prepare receptors for a wide range of templates like drugs, herbicides, sugars, nucleotides, amino acids and protein without appreciably changing the synthetic protocols. Such highly appealing physical and chemical characteristics make MIPs very promising candidates for many applications, including chromatographic stationary-phase [4] and solid-phase separation [5], antibody mimics (biomimetic assays and sensors) [6], enzyme mimics [7], organic synthesis [8], capillary electrochromatography [9], and drug delivery [10].

Acetobacter xylinum, a gram-negative bacterium produces cellulose extracellularly. This cellulose is formed as gel-like mass (pellicle) at the surface of the medium and can be purified by proper chemical treatments. This material has high crystallinity and large surface area [11]. When purified and dried on a flat substrate, a thin translucent cellulose membrane is formed that possess very fine and continuous crystalline microfibrils (not like paper sheets or regenerated cellulose films). Cellulose fibers are relatively strong, having breaking strengths of up to 1 GN/m^2 (10 000 MPa). Cellulose membranes have been widely used as dialyzers for hemodialysis and also used as mechanical support of composite membrane with satisfied mechanical properties for fast protein purification [12]. However, cellulose membranes offer a poor binding capacity due to crystalline and amorphous regions in their structure; only the hydroxyl groups in the amorphous region and on the surface of the crystalline are available to ligand coupling. Molecularly imprinting polymers is implemented to enhance and improve cellulose's mechanical and chemical properties.

Chitosan and chitin membranes have been investigated in order to have a high protein binding capacity for protein purification and separation [13]. These materials provide an excellent binding capacity because chitosan

molecules have both amino and hydroxyl groups that can be used to couple with ligands under mild conditions. But their poor mechanical properties prevented them from being used widely. In order to develop a membrane with good mechanical and chemical properties, these studies propose to make a theophylline imprinted-bacterial cellulose-chitosan (BCC) composite membrane for protein bioseparation, which combines the advantages of MIP, cellulose and chitosan. Both cellulose and Chitosan are biodegradable, natural materials and very abundant on the earth. They also have good blood compatibility [14].

This study aims to develop a composite membrane of bacterial cellulose-chitosan grafted with theophylline-imprinted copolymer and characterize its physical and chemical properties and to evaluate the performance of the developed membrane in ultra-filtration process.

EXPERIMENTAL

Microbial Strains and Chemicals

Pineapple waste juice is supplied by Lee Pineapple Co. Ltd, Malaysia. *Acetobacter xylinum* Culture is obtained from MARDI, Malaysia. Sodium *N,N*-diethyldithiocarbamate trihydrate (EDMA), methacrylic acid (MAA), 4-chloro-methylphenyl-trimethoxysilane, *N,N*-dimethylform-amide (DMF), theophylline, acetic acid, citric acid, polyethylene glycerol, sodium chloride and sodium hydroxide are purchased from Aldrich Chemical Company. Yeast extract and peptone are obtained from Difco Laboratories. Sucrose, glucose, glycerol, ethanol and toluene are supplied by Merck Chemicals.

Culture Media and Method

Cellulose membrane is obtained by incubating *Acetobacter xylinum* in pineapple waste juice supplemented with 4% sucrose (w/v) at pH 5.0. A stainless steel round shallow tray of 39 cm diameter is used to grow the cellulose-producing bacteria at 30°C at the surface of culture medium under static conditions. The culture volume is 500 ml and the effective area from membrane growth is 20 cm^2. Buffered Schamm and Hestrin's medium (BSH medium) is employed as the pre-culture medium, composed of 2.0% (w/v) glucose, 0.5% (w/v) yeast extract, 0.5% (w/v) peptone, 0.033% (w/v) $Na_2HPO_4 \times 2H_2O$ and 0.11% (w/v) citric acid$\times H_2O$. *Acetobacter xylinum* is grown in 50 ml of BSH medium for 3 days to use as pre-culture. The pellicles of bacterial cellulose formed on the

surface of this medium surface are harvested aseptically (21). The harvested pellicle is rinsed with distilled water and soaked in 1% (w/v) NaOH at 80°C for 24 hours and then thoroughly washed with distilled water to remove any remaining associated microorganisms and proteins. The pure cellulose sheets are dried at 37°C overnight and kept in a dust free atmosphere until required for use.

Preparation of the BCC Composite Membrane

The BCC membranes are prepared by phase-inversion method with polyethylene glycerol as the porogen [15]. The chitosan solution with optimized percentage (w/v) of chitosan and optimized percentage (w/v) of polyethylene glycerol (will be obtained via analysis of effect of chitosan and porogen experiments) in a 1% (v/v) aqueous acetic acid solution is obtained. The chitosan solution is filtered by a fritted silica glass Buchner filter of pore size of 40-60 μm and treated in ultrasonic cleaner for 1 hour to remove undissolved substances and air bubbles. Chitosan coating on bacterial cellulose membrane is prepared as follows: the chitosan solution is first flushed through the bacterial cellulose membrane, which is subsequently soaked in the chitosan solution overnight. About 6.5 ml chitosan solution is then poured onto bacterial cellulose membrane placed in a petri dish (100 mm, diameter) and allowed to evaporate at optimized hour (will be obtained via analysis) at ambient temperature. Subsequently, the membrane is immersed overnight in 1 M NaOH to extract the porogen and form a microporous membrane. The resulting composite membrane is washed with large amount of water until the washing solution turned to be neutral and then it is treated with 10% glycerol solution before drying in air to avoid shrinking.

Preparation of the MIP-BCC Composite Membrane

The grafting procedure of ethylene glycol dimethylacrylate (EDMA) and methacrylic acid (MAA) onto regenerated cellulose membrane is using immobilized photoactive iniferter [16]. Chrolomethylbenzyl groups are introduced to the surface of BCC composite membrane by silane coupler (10% (w/w) solution of 4-chloromethylphenyltrimethoxysilane in toluene treated at 353K for 4 hours. This activated membrane is soaked in the ethanol solution of sodium *N*,*N*-diethyldithiocarbamate trihydrate (0.29 M) over 18 hours, then the photoactive iniferter is formed on the surface of the membrane. MAA, EDMA, theophylline are used as a functional monomer, crosslinking monomer and template, respectively. MAA 1.2 g (13.9 mmol), EDMA 12.3 g (62.1 mmol), and theophylline 0.63 g (3.5 mmol) are dissolved in

33 ml of *N*,*N*-dimethylformamide (DMF). The iniferter-immobilized membrane is soaked in the solution of monomer and template, and then irradiated by UV with a germicidal lump (peak intensity at 254 nm) for 1 to 48 hours to cause radical copolymerization. This membrane is ultrasonicated in distilled water for 1 hour in order to remove weakly adsorbed copolymer and to extract theophylline. The membranes are stored in 0.5moldm^{-3} NaCl until characterization.

Characterization of Membranes

Fourier Transform Infrared Spectroscopy (FTIR)

FTIR spectroscopy was used primarily to identify the chemical structure of the membrane. The FTIR spectra of the membranes were measured at wave numbers ranging from 450 - 4000 cm^{-1} with a Perkin Elmer Spectrum One FTIR Spectrometer.

Brunauer-Emmett-Teller (BET) Surface Analysis

The pore size and surface area of the membranes were determined with a BET surface area analyzer. To remove moisture from the film samples, the samples were placed in sample cells, which were then heated up to 373 K for 2 h and cooled down to room temperature before the BET analysis. The BET pore size and surface area were determined with N2 adsorption at 77 K in a Micromeritics (Atlanta, GA) ASAP 2020.

Tensile Property Testing

All the membranes under the study in dry and re-swollen forms were tested for tensile strength, Young's modulus and elongation at break. In the measurement, the crosshead speed is 0.5 cm min^{-1} and 2 × 5 cm dumb bells are tested in a flat-faced grip, initially set 2 cm apart [17]. The maximum tensile strength and break strain of the films were determined with Instron® (Southampton, UK) Model 5567 universal testing machine. The test conditions followed ASTM method D-882-79. The tensile strength and break strain were the average values determined from 10 specimens.

Scanning Electron Microscopy (SEM)

The films were frozen in liquid nitrogen, immediately snapped, vacuum-dried and then sputtered with gold and photographed. Images were taken on a Hitachi S-4700 (Tokyo, Japan) scanning electron microscope.

Membrane Performance Analysis

Flow Rates of Pure Water Measurement

The developed membrane was used in ultrafiltration system to measure the flow rate. The typical setup employed a 70 mm membrane filter holder. The magnetic stirrer was set at 350 rpm and the flow was driven with a peristaltic pump set at 0.35mL min^{-1}. The relationship between the flow rate and the pressure drop is measured via a membrane filter holder, which can hold one piece of membrane with an effective diameter of 55 mm. Pure water is pumped through the membrane holder in a pressure range of 0 to 12.5 psi. The flow rate of water or flux through each membrane is recorded at pressures of 2.5, 5.0, 7.5, 10.0 and 12.5 psi.

Determination of the Weight Ratio of Monomer

The weight ratio of monomer to bacterial cellulose-chitosan membrane is defined as r and calculated according to the following equation:

$$r = (C_{MAA} \times V_{MAA} \times \rho/100)/ W_{membrane} \quad (1)$$

where C_{MAA} is the concentration of methacrylic acid solution, V_{MAA} is the volume of MAA solution, ρ is the density of concentrated MAA and $W_{membrane}$ is the weight of bacterial cellulose-chitosan membrane.

Degree of Grafting

The degree of grafting is determined by gravimetry as the percentage of weight increase of the bacterial cellulose-chitosan. The membranes are weighed before (W_o) and after the grafting process (W_g) and applied the following equation [18]:

$$\text{Degree of grafting (\%)} = [(W_g - W_o)/ W_o] \times 100\% \quad (2)$$

where W_g and W_o are the weights of grafted and ungrafted bacterial cellulose membrane respectively.

Degree of Swelling

Degree of swelling measurements are carried out by immersing clean and dried membrane samples in deionized water until swelling equilibrium is reached. The ungrafted and grafted bacterial cellulose-chitosan membrane is cut into pieces (1 x 2 cm^2) and weighed. After immersing, the excess of

water adhering to the surface is quickly wiped by absorbent paper and then membrane samples are weighed. The degree of swelling is calculated according to the following equation [18]:

$$\text{Degree of Swelling (\%)} = [(W_w - W_d)/ W_d] \times 100\% \quad (3)$$

where, W_w and W_d are the weights of wet and dried membranes respectively.

Evaluation of Living Functionality on Synthesized Copolymer

The relationship between the grafting degree and the number of the repeated grafting cycles is investigated according to similar procedures described in [16]. A piece of MIP-bacterial cellulose-chitosan membrane (5 cm × 5 cm) is prepared by UV irradiation for 2 hours. In total 20 samples of MIP coated membrane sheets were prepared, ultrasonicated in water for 1 hour and dried in vacuum at room temperature. The change in weight as a result of grafting was measured by microbalance AEG-45SM (Shimadzu Corp., Kyoto, Japan: capacity 45 g, readability 0.01 mg). Those procedures are repeated five times.

RESULTS AND DISCUSSION

Characterization of Membranes

Surface Morphology

Figures 1, **2** and **3** shows the FESEM image of the membranes surface at different stages while the cross sections of both membranes are shown in **Figure 4a** and **b**. The lamella-like layers of fibrils in bacterial cellulose membrane still exists in its MIP coated membrane. The membrane developed a denser structure with chitosan and methacrylic acid polymerization. The images showed that many pores in the bacterial cellulose membrane were preserved, leading to lower permselectivity due to co-ions leakage through the membrane. After coating with chitosan, the pores of bacterial cellulose were partially filled as the chitosans were covered to bacterial cellulose. After MIP process with UV irradiation, the pores of bacterial cellulose-chitosan were partially filled as the methacrylic acid were bonded to bacterial cellulose-chitosan. The pores could hardly be observed in the dense structure of the MIP treated BCC membrane. Accordingly, the membrane rejected co-ions (Cl^-), resulting in the increasing permselectivity. By adding 0.5% chitosan, the obtained membranes were significantly denser as demonstrated in **Figure 4**.

The MIP-BCC membranes were thicker and denser related to the chitosan content.

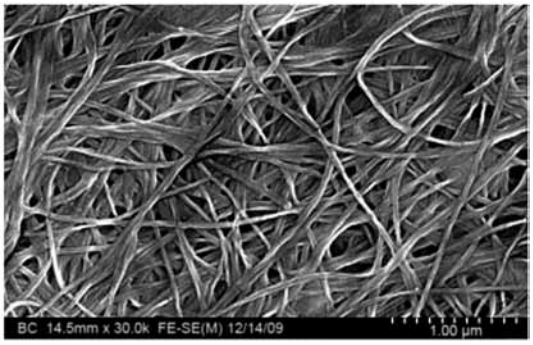

***Figure 1**. The FESEM of the surface of bacterial cellulose membrane*

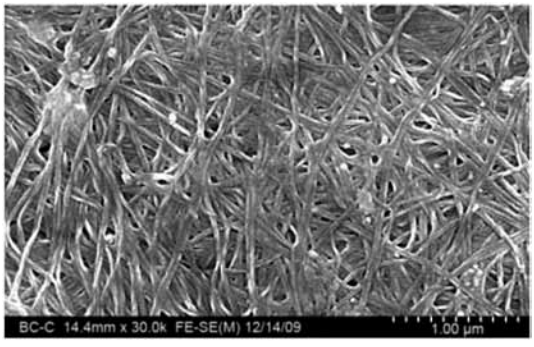

***Figure 2**. The FESEM of the surface of bacterial cellulose-chitosan membrane*

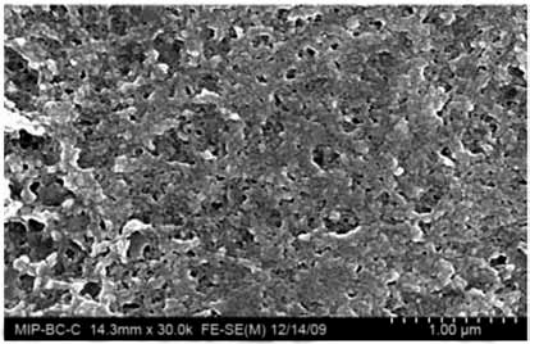

***Figure 3**. The FESEM of the surface of MIP- bacterial cellulose-chitosan membrane*

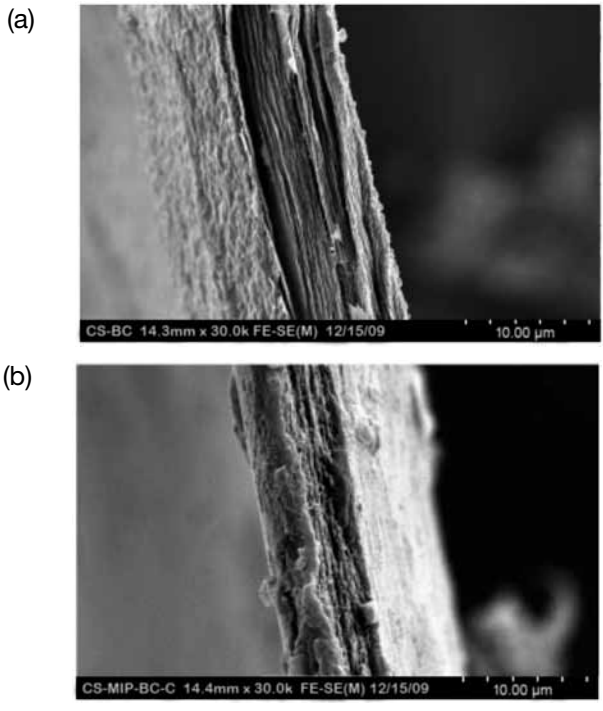

Figure 4*. The FESEM of the cross-section of bacterial cellulose (a) and MIP- bacterial cellulose-chitosan (b) membrane*

Atomic Force Microscopy (AFM) Analysis

The AFM can be used to image and manipulate atoms and structures on a variety of surfaces. The atom at the apex of the tip "senses" individual atoms on the underlying surface when it forms incipient chemical bonds with each atom. Because these chemical interactions subtly alter the tip's vibration frequency, they can be detected and mapped. The AFM provides a true three-dimensional surface profile. Additionally, samples viewed by AFM do not require any special treatments (such as metal/carbon coatings) that would irreversibly change or damage the sample.

AFM images of the membrane in the absence and presence of MIP are shown in **Figure 5a** and **b**. The MIP-BCC composite membrane is clearly rougher in the presence of imprinted theophylline than without imprinted theophylline. The roughening of the MIP surface in the presence of the template can be thought to reflect an increase in the porosity of the MIP. Such an increase in porosity is expected to result in an increase in the permselectivity of the MIP-BCC membrane.

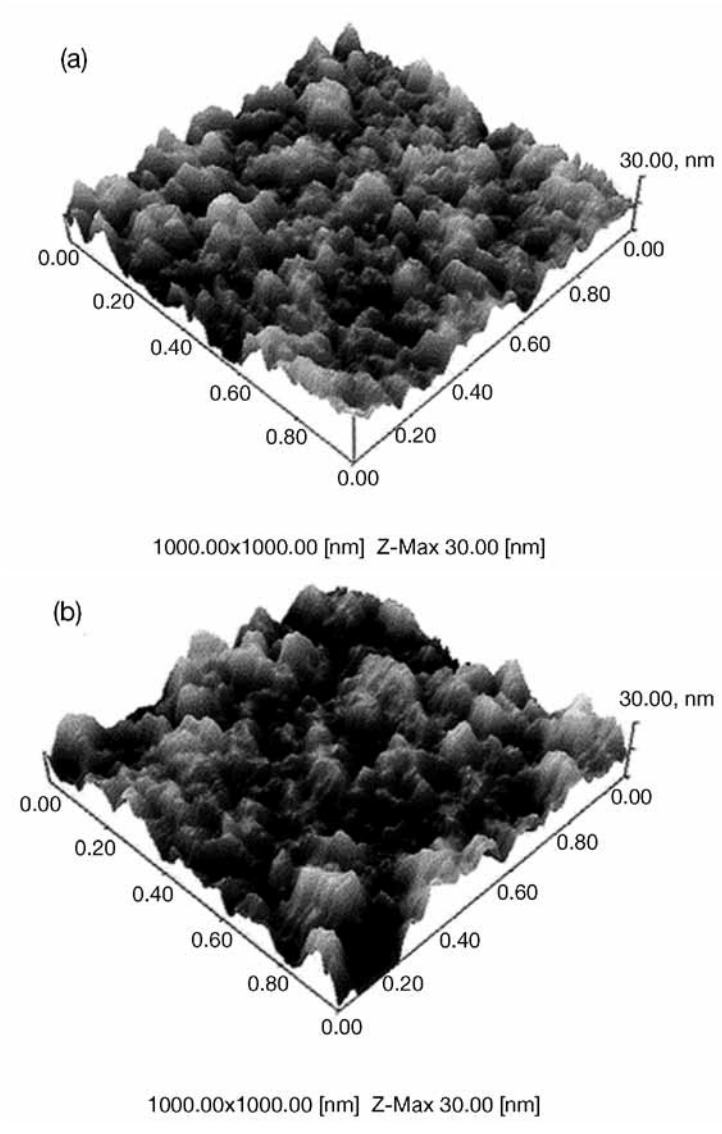

***Figure 5**. The AFM image of BCC (a) and MIP-BCC (b) membrane surface*

FTIR Analysis

Bacterial Cellulose – Chitosan Membrane

FTIR spectroscopy has often been utilized as a useful tool in determining specific functional groups or chemical bonds that exist in a material [19].

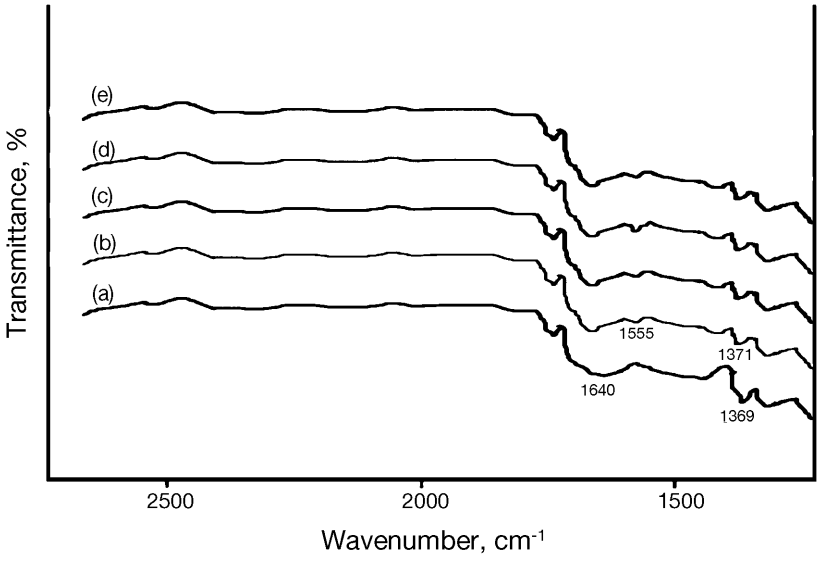

***Figure 6**. The FTIR spectra of BCC membranes in the wave numbers ranging from 2800 to 1200 cm^{-1}*

Figure 6 as shown below demonstrated the FTIR spectra of BCC membranes in the wave numbers ranging from 2800 to 1200 cm^{-1} to show bands for amide group. The supplements of chitosan (% w/v) in BCC were (a) 0.00%, (b) 0.25%, (c) 0.40%, (d) 0.50% and (e) 0.75% which existed in chitosan molecule, appeared around wave number 1375, 1560 and 1650 cm^{-1} and a band at around 1640 cm^{-1}, which was attributed to glucose carbonyl of cellulose. The expansion of the FTIR spectra of BCC membrane at wave number ranging from 1800 to 1500 cm^{-1} in **Figure 7** demonstrated the adsorption bands at around 1640.5 cm^{-1} and around 1555– 1558 cm^{-1}. The intense absorption in the spectrum of the cellulose was the band at 1640.5 cm^{-1}, which was mostly assigned to glucose carbonyl of cellulose as shown in **Figure 7a**. The characteristic absorption of the chitosan was the band at 1557.5 cm^{-1}, which was assigned to the amino groups of chitosan as shown in **Figure 8b**. In addition, the intensity of this band increased gradually with chitosan content. The results suggested that intermolecular hydrogen bonding interaction took place between cellulose and chitosan, leading to a good miscible membrane.

A similar observation was described earlier in blends of chitosan with two cellulose ethers–hydroxypropylmethylcellulose and methylcellulose by casting from acetic acid solutions. It has been proposed that the intermolecular hydrogen bonding of cellulose was broken down to form cellulose–chitosan hydrogen bonding; on the other hand, the intra- molecular and intra-strand

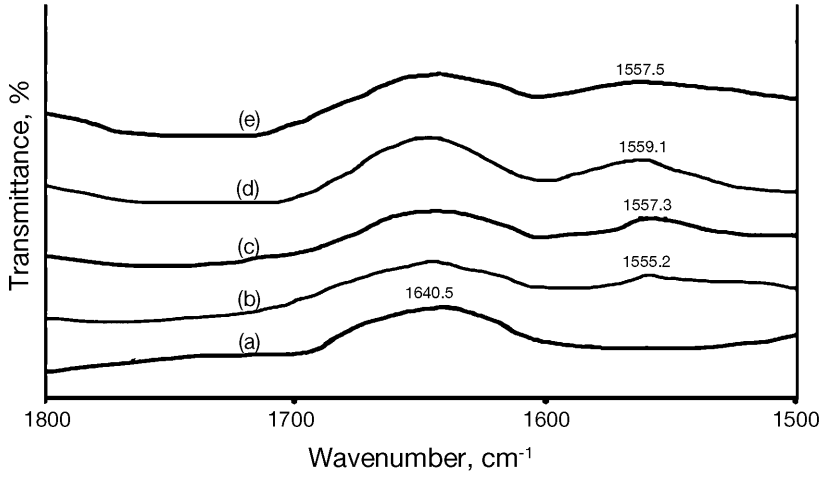

***Figure 7**. The FTIR spectra of BCC membranes in the wave numbers ranging from 1800 to 1500 cm^{-1}*

hydrogen bonds held the network flat [21]. With the introduction of chitosan into the cellulose material, there was a strong interaction between chitosan and cellulose, and a lot of hydrogen bonds, ionic bonds and a few covalent bonds were presented [22, 23, 24].

Theophylline Imprinted-Bacterial Cellulose-Chitosan Membrane

The FTIR spectra of the optimized BCC membrane and the MIP –BCC membrane prepared under the optimal conditions are shown in **Figure 8**. **Figure 8a** shows that the main characteristic peaks of bacterial cellulose-chitosan are at 3444 cm^{-1} (O–H stretch), 2878 cm^{-1} (C–H stretch), 1600 cm^{-1} (N–H bend), 1325 cm-1 (C–N stretch), 1155 cm^{-1} (bridge O stretch), and 1090 cm^{-1} (C–O stretch). In **Figure 8b** the spectrum of MIP membrane, in addition to the bacterial cellulose-chitosan characteristic peaks, some new absorption peaks appear. The peak at 1720 cm^{-1} corresponds to the carboxyl absorption from grafted poly (methacrylic acid) and the peaks at 810 and 620 cm^{-1} are also characteristic of poly (methacrylic acid) [22, 25]. Furthermore, the bands at 1560 and 1400 cm^{-1} correspond to the sodium carboxyl group. These indicate that methacrylic acid in polymer has been grafted onto bacterial cellulose-chitosan membrane.

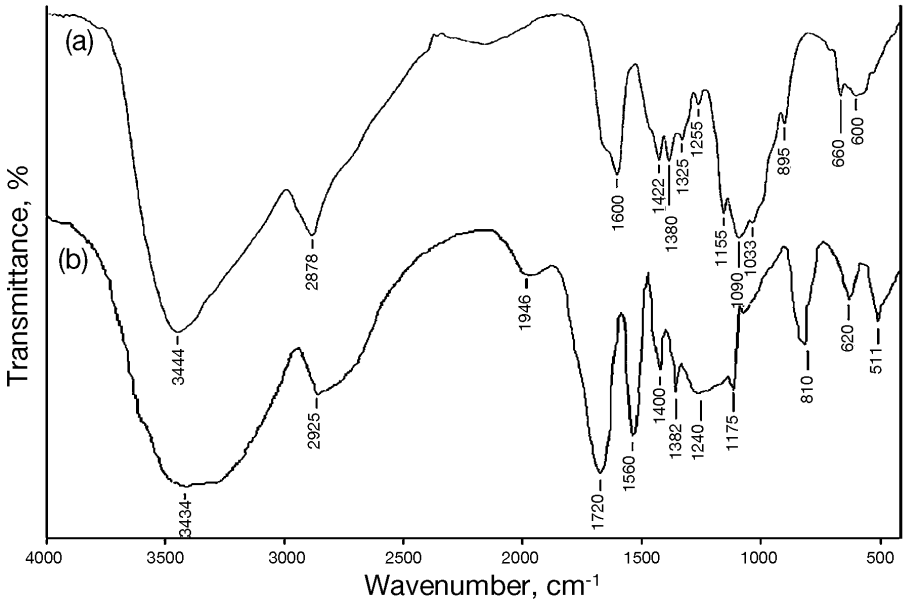

***Figure 8**. The FTIR spectra of the BCC (a) and MIP-BCC (b) membranes*

Mechanical Property

The mechanical property of the membrane is another important factor when used for membrane separation. **Figure 9** shows the effects of chitosan addition on the tensile strength of the membranes. The blank sample of the BC membrane is the sample with 0% of chitosan content. In comparison to that of the BC membrane, the tensile strength of BCC membrane increased with an increase of chitosan content. The maximum tensile strength of the dry membrane with an average thickness of 0.037 mm was 16 MPa after adding 0.75% (w/v) chitosan of MW 30,000 respectively. The tendency of tensile strength of the re-swollen (wet) membrane rather corresponded to the dry membranes but in a lower range. The maximum average value of the wet membrane was 2.16 MPa after 0.75% (w/v) additions of chitosan of MW 30,000 respectively. The tensile strength of the dry BCC membrane was relatively higher than that of BCC membrane in the wet state due to the swelling of cellulose fiber and chitosan in an aqueous solution. The tensile strength of the composite membranes coated with different chitosan concentrations is larger than the plain bacterial cellulose membrane. It is because the cellulose fiber becomes thicker after being coated with chitosan which improves mechanical properties. In addition, a chitosan network is formed between cellulose fibers in the composite membrane; the pull force on the cellulose fiber would be

distributed on the chitosan network [25]. The fiber in the composite membrane would then withstand a stronger pull force than the cellulose fiber alone. One can also see that the strength of the composite membrane in wet state is much lower than that in dry state; this is due to the swelling of cellulose fiber and chitosan in aqueous solution. The strengths of chitosan–cellulose composite membranes in both dry and wet state, however, are higher compared with those of chitosan membrane reported in literature [23, 24].

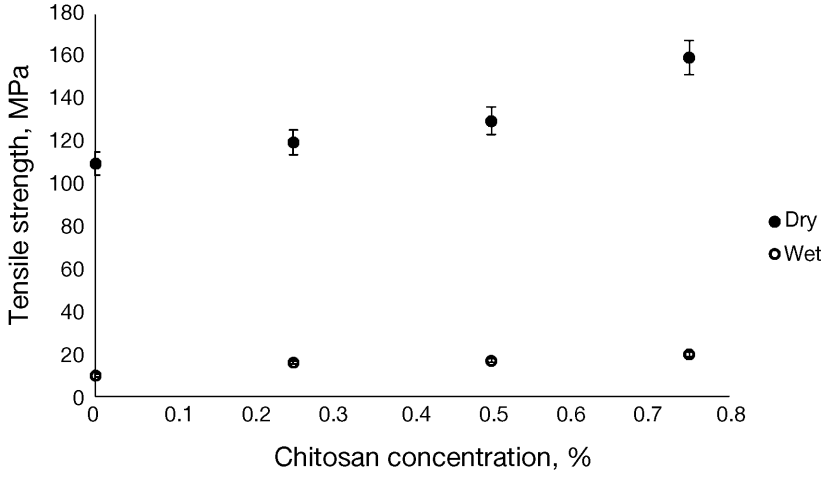

***Figure 9**. Tensile strength of the composite membrane in dry and wet states coated with solution of different concentration containing 15% PEG, evaporation time was 2.5 hours*

Membrane Porosity

The total surface area and average pore size of the entire BC membrane determined by BET were 12.3 m^2/g and 218 Å and in agreement with previous researches [24]. As shown in **Table 1**, BCC membranes with supplementation of 0.5% (w/v) of chitosan (the optimized concentration of chitosan) had pore sizes smaller than those of BC while the surface areas were relatively increased in the later. The pore sizes of the BCC membrane was 156 Å and the pore sizes of the MIP-BCC membrane was 135 Å, with the total surface area of 14.7 and 14.9 m^2/g respectively.

For the re-swollen form, the total surface area and average pore sizes of the BC film were 54.7 m^2/g, and 606 Å, respectively. The pore size of the wet membrane of BCC was 491 Å with the total surface area of 83.1 m^2/g, respectively while the pore size of the wet membrane of MIP-BCC was 404 Å

Table 1. Average pore size and surface area of the BC, BCC and MIP-BCC analyzed with BET analyzer

State	Membrane	Average Pore Diameter (Å)	Surface Area (m^2/g)
Dry	BC	218	12.3
	BCC	156	14.7
	MIP-BCC	135	15.1
Wet	BC	606	54.7
	BCC	491	83.1
	MIP-BCC	404	98.8

with the total surface area of 98.8 m^2/g, respectively. This result was in good agreement with the observation from FESEM micrograph. It was found that the additional chitosan of the composite bacterial cellulose–chitosan membrane resulted in the formation of denser matrix networks, higher surface area and smaller pore diameter [15]. The average pore size determined by BET was much smaller than those on the surface observed from the SEM images. Therefore, the pores inside the film should be smaller than those on the surface.

Degree of Grafting

The effect of the free radical copolymerization on degree of grafting of methacrylic acid onto bacterial cellulose-composite membrane is shown in **Figure 10**. The degree of grafting increases with increasing of number of

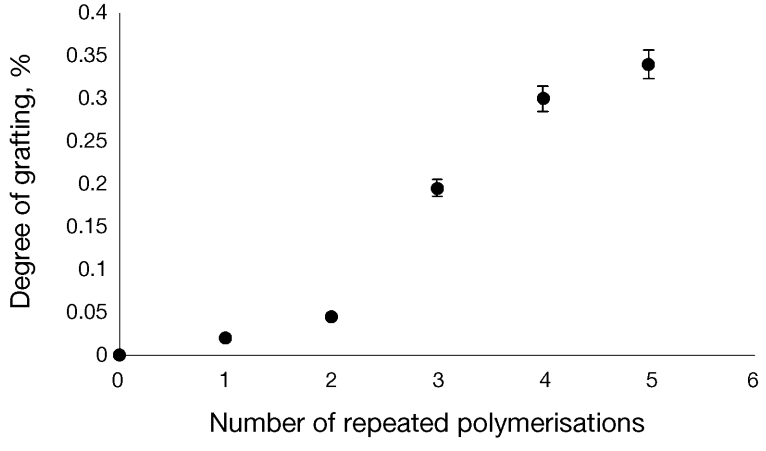

***Figure 10**. Effect of repetition of polymerization on degree of grafting*

repeated polymerizations. Using a free radical copolymerization, the highest degree of grafting obtained was 0.3334% for r (weight ratio of monomers to bacterial cellulose-chitosan membrane) equal to 3.244 in mmol/ml, respectively. It means that increasing number of repeated polymerizations gave higher degree of grafting due to higher amount of methacrylic acid supplied for copolymerization reaction. Consequently, the increased amount of monomer led the methacrylic acid to diffuse more into polymer matrix resulted in higher probability of collision between monomers and polymer radicals.

Degree of Swelling

The degree of grafting effect on the degree of swelling of MIP composite membrane is presented in **Figure 11**. The degree of swelling of non-MIP composite membrane itself was 12.5% and it increases significantly with the increase of degree of grafting. This result showed that the resulting copolymer has higher hydrophilicity properties. The incorporation of more –COOH groups from methacrylic acid to the membrane is believed to occur with the increase of the degree of grafting and caused higher hydrogen bonding between grafted methacrylic acid groups and water. According to previous study, for the same degree of grafting, the grafted membrane with lower r value shows a degree of swelling remarkably higher than higher r value [25].

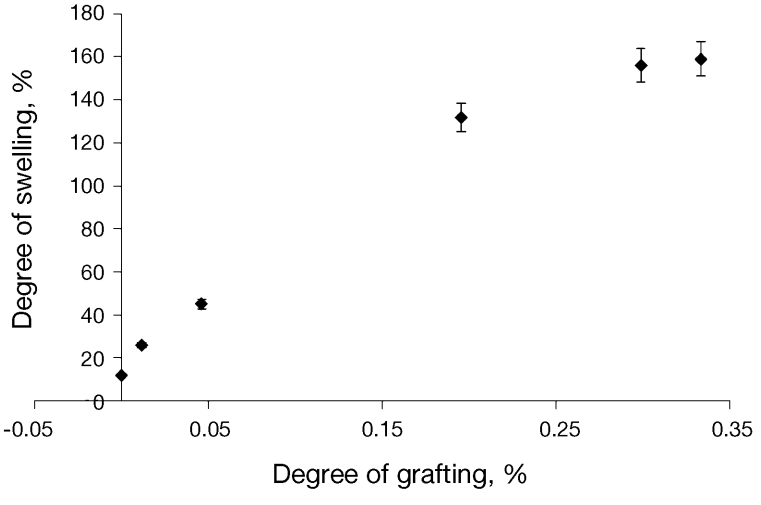

***Figure 11**. Effect degree of grafting on degree of swelling*

Membrane Separation Properties

The permeability of both non-MIP and MIP composite membrane are shown in **Figure 12**. It can be seen that the water flux at fixed pressure (30 psi) decreases with the increase of degree of grafting. Comparing the hydrophilicity of the grafted and the original membrane, one can expect that grafted membranes should have higher water flux.

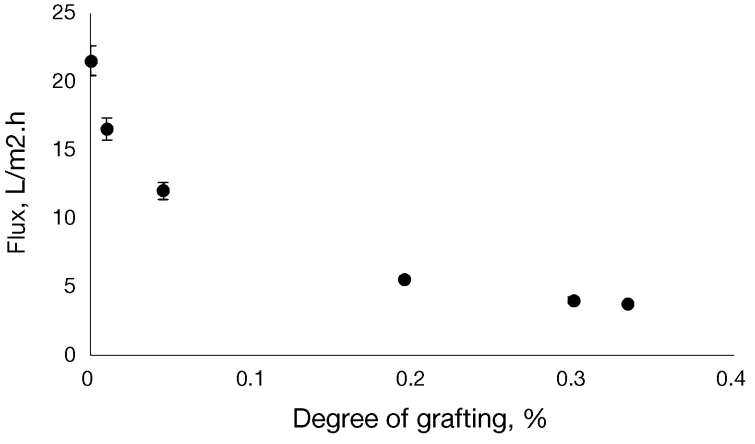

***Figure 12**. Effect of degree of grafting on water flux*

Surprisingly, the results show the opposite effect. It seems that the interaction between the membrane and water become tighter due to the presence of polar groups from methacrylic substituent which build more hydrogen bonds [24]. This membrane-water interaction tends to retain water in the membrane vicinity and hence, it takes more time for water to permeate through the membrane. It was also found that the flux of water was almost the same for degrees of grafting ranging between 0.2989% and 0.3334%. It seems that the existing interaction between membrane and water in those membranes have already achieved their equilibrium and optimized state.

CONCLUSIONS

This research has successfully developed a membrane of bacterial cellulose-chitosan grafted with theophylline-imprinted copolymer and characterized its physical and chemical properties. Free radical copolymerization for the grafting of the imprinted polymer was applied using photoactive iniferter

immobilized on the bacterial cellulose-chitosan membrane. This membrane was modified with methacrylic acid by UV-graft polymerization to prepare ultrafiltration membranes having a selectivity approaching those of antibody antigen systems and greater structural density. The MIP was successfully grafted to membrane surface. The changes of chemical structure were characterized by FTIR spectroscopy which showed a new band at 1720 cm^{-1} attributed to the carbonyl group of methacrylic acid. FTIR spectra showed that MAA was successfully bound to the bacterial cellulose membrane. FE-SEM photographs showed that the MIP-BCC membrane was morphologically dense as MAA was bound to bacterial cellulose-chitosan composite membrane. The surface of MIP-BCC membrane is clearly rougher in the presence of imprinted theophylline than without imprinted theophylline as evaluated by AFM images. The developed membrane exhibited excellent mechanical properties due to the crystalline structure of the bacterial cellulose. Further improvement in the permselectivity may be achieved by selection of modifying monomers or chemical treatment and/or morphological control of membranes.

REFERENCES

1. Vriezema D., Aragones M., Elemans J., Cornelissen J., Rowan A. and Nolte R., *Chemical Reviews*, **105** (2005), 1445-1490.
2. Wulff G., *Chemical Reviews*, **102** (2002), 1-28.
3. Kempe M. and Mosbach K., *Tetrahedron Letters*, **36** (1995), 3563-3566.
4. Turiel E. and Martin-Esteban A., *Analytical and Bioanalytical Chemistry*, **378** (2004), 1876-1886.
5. Haginaka J., *Analytical and Bioanalytical Chemistry*, **379** (2004), 332-334.
6. Haupt K., *Chem. Commun.* **2** (2003), 171-178.
7. Ramström O and Mosbach K., *Curr. Opin. Chem. Bio.,* **3** (1999), 759-764.
8. Alexander C.L. and Hayes W., *Tetrahedron,* **59** (2003), 2025-2057.
9. Spégel P., Schweitz L., and Nilsson S., *Electrophoresis*, **24** (2003), 3892-3899.
10. Alvarez-Lorenzo C. and Concheiro A., *J. Chromatogr. B.,* **804** (2004), 231-245.
11. Shibazaki H., Kuga S., Onabe F., and Usuda M., *Journal of Applied Polymer Science*, 50 (1993), 965-969.
12. Hou K.C., Zaniewski R., and Roy S., *Biotechnol. Appl. Biochem.,* **13** (1991), 257-262.

13. Zeng X. and Ruckenstein E., ***Biotechnol. Bioeng.,* 56** (1997), 610-617.

14. Jia L., Yang L., Zou H., Zhang Y., Zhao J., Fan C., and Sha L., ***Biomed. Chromatogr.,* 13** (1999), 472-479.

15. Yang L., Hsiao W.W. and Chen P., ***Journal of Membrane Science,* 197** (2002), 185-197.

16. Hattori K., Hiwatari M., Iiyama C., Yoshimi Y., Kohori F., Sakai K., and Piletsky S.A., ***Journal of Membrane Science,* 233** (2004), 169-173.

17. Choi Y.J., Ahn Y., Kang M.S., Jun H., Kim I.S. and Moon S., ***Journal of Chemical Technology and Biotechnology,* 79** (2004), 79-84.

18. Pawlak A. and Mucha M., ***Thermochimica Acta,* 396** (2003), 153-166.

19. Lee Y.M., Kimt S.H., and Kimt S.J., ***Polymer,* 37** (1996), 5897-5905.

20. Yin J., Luo K., Chen X., and Khutoryanskiy V.V., ***Carbohydrate Polymers,* 63** (2006), 238-244.

21. Wu Y.B., Yu S.H., Mi F.L., Wu C.W., Shyu S.S., and Peng C.K., ***Carbohydrate Polymers,* 57** (2004), 435-440.

22. Fu L.H. and Cheng J.Q., ***Zhongguo Zaozhi Xuebao/Transactions of China Pulp and Paper,* 21** (2006), 48–51.

23. Urreaga J. M. and de la Orden M.U., ***European Polymer Journal,* 42** (2006), 2606-2616.

24. Phisalaphong M., Suwanmajo T., and Sangtherapitikul P., ***Journal of Applied Polymer Science,* 107** (2008), 292-299.

25. Yang L. Hsiao W.W. and Chen P., ***Journal of Membrane Science,* 197** (2002), 185-197.

GRAPHICAL ABSTRACT